Lumped Dynamic Analysis and Design of a High-Performance Reciprocating-Piston Expander

Paul Sapin[a], Michael Simpson[b], Alexander J. White[c] and Christos N. Markides[d]

[a] Clean Energy Processes (CEP) Laboratory, Department of Chemical Engineering, Imperial College London, London, UK, p.sapin@imperial.ac.uk
[b] Clean Energy Processes (CEP) Laboratory, Department of Chemical Engineering, Imperial College London, London, UK, m.simpson16@imperial.ac.uk
[c] Cambridge University Engineering Department, Trumpington Street, Cambridge, UK, ajw36@cam.ac.uk
[d] Clean Energy Processes (CEP) Laboratory, Department of Chemical Engineering, Imperial College London, London, UK, c.markides@imperial.ac.uk (CA)

Abstract:

A spatially-lumped dynamic model of a reciprocating-piston expander is presented in this paper. The model accounts for the three main loss mechanisms in realistic piston machines, namely: pressure losses through the intake and exhaust valves, heat transfer between the gas and the surrounding cylinder walls, and the mass leakage between the compression/expansion chamber and the crankcase through the piston rings. The model also accounts for real-gas effects with the fluid properties calculated from the NIST database using REFPROP. The numerical calculations are first compared with experimental pressure-volume-temperature data obtained on a custom reciprocating-piston gas spring over a range of oscillation frequencies. The comparison between numerical and experimental results shows good agreement. It also allows the most accurate heat transfer correlation to be selected for calculating the gas-to-wall in-cylinder heat transfer. The semi-heuristic modelling tool is then used to design an expander for specific pressure ratios and mass flowrate, and to predict the thermodynamic performance of the piston device over a range of part-load conditions.

Keywords:

Expander design; Reciprocating piston; Real gas effects; Heat and mass losses; Thermodynamic performance.

1. Towards a sustainable and clean energy future

The generation of energy from renewable sources and the recovery and utilisation of waste heat are two important pillars of the transition towards a sustainable, clean energy future. Amongst other energy conversion technologies, Organic Rankine Cycle (ORC) engines can be used to harness the potential of these alternative energy sources. The thermodynamic performance of such technologies depends significantly on the expander efficiency. At the same time, the integration of intermittent energy sources into the existing energy systems requires intermediate- to large-scale energy storage technologies, for example Compressed-Air Energy Storage (CAES) or Pumped-Thermal Electricity Storage (PTES) [1]. As with ORC systems, the design and selection of the compression/expansion devices is key in optimising the overall performance of these technologies.

At small scales (1-10s kW), positive displacement machines such as scroll or screw expanders are usually chosen because they can achieve high isentropic efficiencies when operated near a selected rating point. However, their efficiency decreases at high pressure ratios. Turbomachines are preferred for large power applications (>100 kW). Reciprocating-piston devices are proposed because they have a potential for higher efficiencies at intermediate scales (~10s-100s kW) and are mass produced, affordable and robust. Furthermore, reciprocating-piston expanders and compressors can maintain good efficiencies at partial loads.

The thermodynamic performance of such devices is affected by four loss mechanisms, namely: pressure losses through the valves, heat losses, mass leakage and friction between the solid moving-parts, which with good lubrication becomes negligible in comparison with the others. The pressure losses during the intake and exhaust strokes depend on the valve design and timing. The mass leakage and heat transfer are more complex, however. During the expansion and compression strokes,

unsteady gas-to-wall in-cylinder heat transfer and mass leakage between the crankcase and the compression/expansion chamber through the piston rings take place, inducing exergetic losses that need to be predicted accurately if high-efficiency devices are to be designed.

This paper presents a lumped model of a reciprocating-piston expander accounting for the three main loss mechanisms, pressure losses through the valves, heat losses and mass leakage as aforementioned. The model is first compared to a set of experimental data measured on a gas spring (*i.e.* without valve system) operated at various oscillation frequencies. Cyclic-loss parameters are defined to estimate both the contributions of heat losses and mass leakage. The comparison between the computed and experimentally measured losses show good agreement and allow us to select the most reliable heat transfer correlation to be used in the model. Finally, the model is used to calculate the performance map of a reciprocating-piston expander for different pressure ratios, using an organic fluid as a working fluid, namely the refrigerant R245fa.

Nomenclature

Latin characters		
A_{gap}	Piston ring gap area	[m^2]
A_{R}	Valve restriction area	[m^2]
A_{w}	In-cylinder wall area	[m^2]
c_{p}	Isobaric specific heat capacity	[J/(kg.K)]
C_{d}	Discharge coefficient	[-]
D_{h}	Hydraulic diameter	[m]
h	Specific gas enthalpy	[J/kg]
k	Thermal conductivity	[W/(m.K)]
m	Mass of gas in the control volume	[kg]
$\dot{m}$	Mass flow rate	[kg/s]
Nu	Nusselt number	[-]
P	Pressure	[Pa]
Pe_{ω}	Oscillatory Péclet number	[-]
$\dot{Q}_{\mathrm{w}}$	Gas-to-wall heat flux	[W]
$\dot{q}_{\mathrm{w}}$	Gas-to-wall heat flux density	[W/m^2]
Q_{loss}	Net cyclic heat loss	[J]
S	Specific entropy	[J/(kg.K)]
T	Temperature	[K]
T_{line}	Line-averaged temperature	[K]
V	Volume	[m^3]
v	Fluid velocity	[m/s]
W_{loss}	Net cyclic work done on the gas	[J]
$\dot{W}$	Output power	[W]
Greek characters		
α_{m}	Cyclic-mean thermal diffusivity	[m^2/s]
η	Expander efficiency	[-]
η_{vol}	Volumetric efficiency	[-]
θ	Crank angle	[rad]
ρ	Density	[kg/m^3]
ψ_{therm}	Non-dimensional cyclic thermal loss	[-]
ψ_{total}	Non-dimensional cyclic work loss	[-]
ω	Angular frequency	[rad/s]

2. Modelling methodology

The full thermo-fluid problem of a reciprocating-piston expander is complex and exhibits a wide range of parameters and conditions, that can be solved with Computational Fluid Dynamic (CFD) tools. Yet, CFD is not suitable in the early-design stages as it is a highly time-consuming approach.

The model proposed in this article is based on a dynamic lumped system analysis (as was the model from Mathie *et al.* [2] that solved the conjugate heat transfer problem in gas spring configuration). It provides great simplification without much sacrifice from accuracy. It can be readily used to predict the thermodynamic performance of reciprocating engines (much faster than a fully-resolved CFD simulation), accounting for (i) pressure drops through the valves, (ii), mass leakage through the piston rings and (iii) gas-to-wall heat transfer.

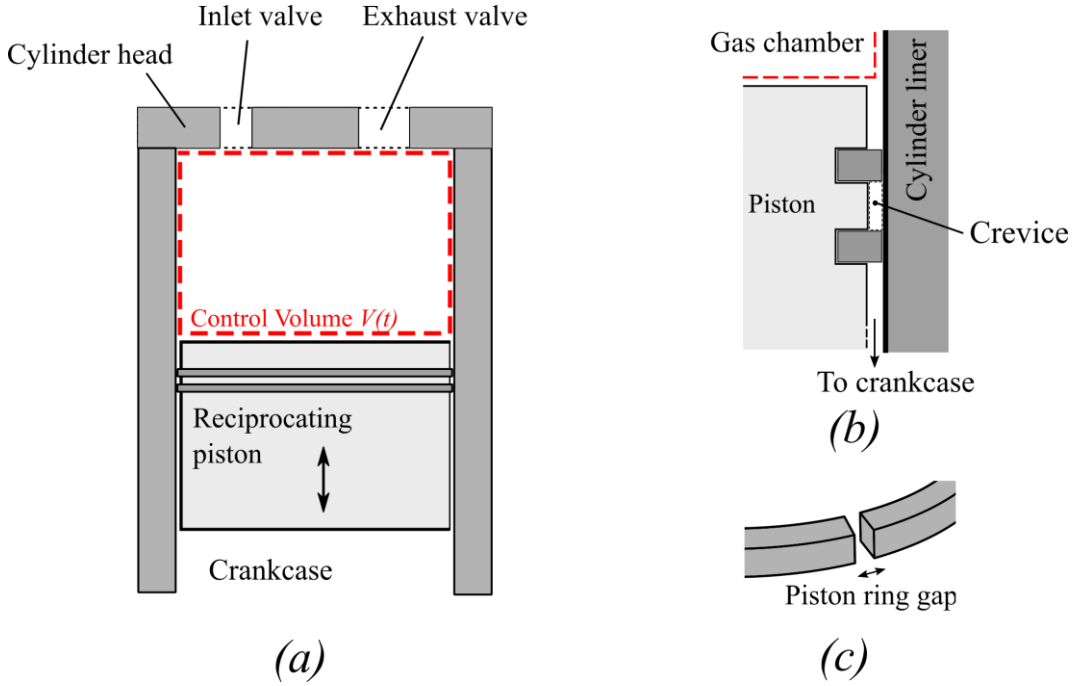

Fig. 1. (a) Reciprocating-piston compressor or expander arrangement and control volume used in the analysis, (b) schematic of the piston ring sealing, (c) schematic of the piston ring gap

2.1. Lumped system analysis

The varying mass of gas contained in the cylinder of a reciprocating-piston device undergoes various thermodynamic processes. In the present analysis, the gas in the cylinder is considered to behave like a "lump", with temperature, T, pressure, P, and density, ρ, fields considered uniform along the cycles. Mass and energy conservation equations (Eqs. (1) and (2)) are solved within a control volume (CV) $V(t)$ that is the in-cylinder volume, as represented in Fig. 1(a).

$$\frac{\mathrm{d}m}{\mathrm{d}t} = \dot{m}_{\mathrm{in}} - \dot{m}_{\mathrm{out}} \,, \tag{1}$$

$$\frac{\mathrm{d}}{\mathrm{d}t}(mh) = \dot{Q}_{\mathrm{w}} + V\frac{\mathrm{d}P}{\mathrm{d}t} + \sum \dot{m}_{\mathrm{in}}\left(h_{\mathrm{in}} + \frac{{v_{\mathrm{in}}}^2}{2}\right) - \sum \dot{m}_{\mathrm{out}}\left(h_{\mathrm{out}} + \frac{{v_{\mathrm{out}}}^2}{2}\right), \tag{2}$$

where $\dot{Q}_{\mathrm{w}} = \dot{q}_{\mathrm{w}}\, A_{\mathrm{w}}$ is the net heat flux, defined as positive if it is transferred from the walls to the gas. The mass exchange terms, $\dot{m}_{\mathrm{in}}$ and $\dot{m}_{\mathrm{out}}$, denote the mass flow rates into and out of the CV, whether through the piston rings or through the intake/exhaust valves.

The equation-of-state (EOS) is to be solved together with the mass and energy conversation equations. In the gas spring experiments presented in section 3, the working fluid is dry air, whose behaviour can be accurately described by the ideal gas EOS. However, the modelling of reciprocating expanders or compressors using organic fluids – with much higher molecular weights – is not accurate under the ideal-gas assumption because of the significant compressibility effects. Hence, the thermo-physical properties of the gas are interpolated from the NIST database using the software REFPROP.

2.2. Pressure losses through valve systems

The gas intake or exhaust through the valves are caused by a pressure difference across the valve restriction (of characteristic area A_{R}). The mass flow rate through valves is usually described by the

compressible flow equation assuming a one-dimensional isentropic flow using a discharge coefficient, C_d, to account for real gas flow effects [3]:

$$\dot{m}_{\mathrm{in/out}} = C_\mathrm{d}\, A_\mathrm{R} \sqrt{2(h_\mathrm{up} - h_\mathrm{R})}\,, \text{ with:} \tag{3}$$

$$h_\mathrm{R} = h\big(P_\mathrm{dn}, S_\mathrm{up}\big)\,, \tag{4}$$

where h_up and S_up are respectively the specific enthalpy and entropy upstream of the flow restriction and P_dn is the pressure downstream of the valve.

2.3. Mass leakage in reciprocating-piston engines

In reciprocating-piston devices, piston rings – or split rings – fit into grooves on the outer diameter of the piston to limit the mass loss to the crank case, as shown in Fig. 1(b). Split rings are not continuous but are broken at one point (see Fig. 1(a)) so that they can be fitted into the grooves. Sealing is achieved by multiple rings – two in our case, yet it still allows blow-by mass leakage through the end gaps.

To estimate this loss mechanism, a mass conservation equation (Eq. (5)) is written for the crevice formed in-between two rings (denoted with the subscript 'crev'). The mass accumulation in the crevice is related to the mass flow rates towards or from the crankcase and the gas chamber:

$$\frac{\mathrm{d}m_\mathrm{crev}}{\mathrm{d}t} = \dot{m}_\mathrm{in,crev} - \dot{m}_\mathrm{out,crev}\,. \tag{5}$$

The mass flow rates in or out the crevice are related to the difference between the upstream specific enthalpy, h_up, and the specific enthalpy at the gap, h_gap. This relation is given by the steady-flow energy-equation assuming isentropic flow (similar to Eq. (3)):

$$\dot{m}_\mathrm{in/out,crev} = C_\mathrm{d}\, \rho_\mathrm{crev}\, A_\mathrm{gap} \sqrt{2(h_\mathrm{up} - h_\mathrm{gap})}\,, \text{ with:} \tag{6}$$

$$h_\mathrm{gap} = h\big(P_\mathrm{dn}, S_\mathrm{up}\big)\,, \tag{7}$$

where $C_\mathrm{d}$is a discharge coefficient that corresponds to the ratio between the effective flow-section area and the gap area, which is estimated with the correlation from Rakopoulos *et al.* [4]:

$$C_\mathrm{d} = 0.85 - 0.25\left(\frac{P_\mathrm{dn}}{P_\mathrm{up}}\right)^2\,. \tag{8}$$

2.4. Instantaneous heat-transfer in reciprocating gas-springs

The gas-to-wall heat transfer in reciprocating-piston compressors or expanders is determined differently depending on the undergoing process. The heat transfer characteristics during the expansion and compression strokes are influenced by the pressure fluctuations while the heat transfer during intake and exhaust is closer to a classical forced-convection gas-to-wall heat transfer.

2.4.1. Heat transfer during compression and expansion processes

The prediction of heat transfer during compression and expansion processes is not straightforward as the heat transfer can be out of phase with the bulk gas-to-wall temperature difference, as first pointed out by Pfriem in 1943 [5]. The conventional Newton's law of cooling, based on the steady-state boundary layer theory, fails at describing this phenomenon and conventional Nusselt-Reynolds correlations are not suitable for this exchange, which was later confirmed by experimental observations [6]. Empirical correlations have been proposed to estimate this complex heat transfer, amongst which the most notable one is this by Kornhauser and Smith [7] based on a complex Nusselt number, *Nu*. More recently, Lekić and Kok [8,9] simulated numerically the heat transfer and fluid flows in valveless gas-springs with a finite-volume CFD code and revealed limitations to the aforementioned correlation for high compression ratios. These authors proposed a modified version

of the Kornhauser and Smith correlation, also based on a complex Nusselt number, *Nu*. In this study, the instantaneous heat transfer between the gas and the wall, considered at constant and uniform temperature, is evaluated from:

$$\dot{q}_{\mathrm{w}} = \frac{k}{D_{\mathrm{h}}}\left[Nu_{\mathrm{r}}(T - T_{\mathrm{w}}) + \frac{Nu_{\mathrm{i}}}{\omega}\frac{\mathrm{d}T}{\mathrm{d}t}\right], \tag{9}$$

where Nu_{r} and Nu_{i} are real and imaginary parts of the complex Nusselt number, respectively. Their values differ between the Kornhauser and Smith (K&S) and Lekić and Kok (L&K) correlations.

2.4.2. Heat transfer during intake and exhaust

During intake and exhaust strokes, it has been chosen to use a conventional formulation with the Nusselt number equal to the real part of the aforementioned correlations:

$$\dot{q}_{\mathrm{w}} = \frac{k}{D_{\mathrm{h}}} Nu_{\mathrm{r}}(T - T_{\mathrm{w}}) \,. \tag{10}$$

In other words, the imaginary part of the complex number is set to zero during these phases as the effect of the pressure fluctuation is negligible.

3. Experimental validation

The model was compared to experimental results from a gas-spring operated at different frequencies. Cycle-resolved measurements of cylinder pressure, temperature and volume were used to trace the mass changes in the cylinder, which could then be compared with model predictions. Thermodynamic losses were calculated for each operating frequency, and cyclic-loss parameters were obtained. The lumped mass model and its assumptions were tested for validity against each of these metrics.

3.1. Experimental methodology

The experimental apparatus is a single-cylinder reciprocating compressor which has been converted into a gas spring (see Fig. 2). The valve arrangement has been removed and replaced by a sealed cylinder head. The bore diameter is 105 mm, the stroke length is 78 mm, the connecting-rod length is 148.5 mm, and the dead volume height is 14 mm. The built-in volume ratio is 6.6. Mass leakage past the piston is limited by a set of piston rings, which sit in grooves on the outer diameter of the piston. An 11-kW 3-phase induction motor powers the rig, and is controlled using a variable-frequency drive. Data are obtained at frequencies from 27 to 300 RPM.

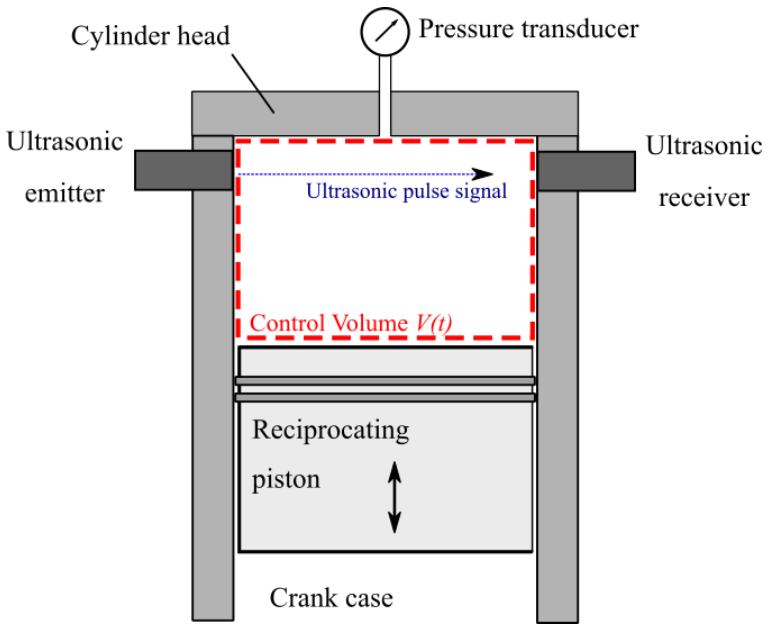

Fig. 2. Gas-spring arrangement and control volume used in the analysis

Measurements are made of bulk pressure, volume and temperature within each cycle. Pressure, *P*, is measured by a pressure transducer (OMEGA PX35D0) situated at the cylinder head. Volume, *V*, is calculated from the instantaneous crank angle, measured by a shaft encoder (BAUMER BMSV30). The gas temperature, *T*, is measured using an ultrasonic system developed in-house. A pulse signal is generated by a piezoelectric ceramic transducer, which travels across the cylinder to a transducer directly opposite. The travel time of the signal is calculated according to Mathie *et al.* [10], from which the speed of sound within the gas is derived and hence the gas temperature. The measurement is therefore a line-averaged temperature of the gas between the transducers.

Before use, the cylinder and crankcase are purged with dry compressed air. The experimental run commences with the piston at top dead centre (TDC) and gas at ambient temperature and pressure. The motor-driven reciprocating motion leads to an initially below-atmospheric average pressure over the cycle, causing a net mass leakage past the piston rings into the cylinder such that the pressure ratio increases over time to a steady-state value.

3.2 Model configuration

In order to model the gas-spring experimental setup, a simple modification to the model was made to fix valve input/output flow to zero. Gas-to-wall heat transfer and mass leakage past the piston rings remained as sources of loss within the model. The heat transfer was predicted using correlations available in the literature from Kornhauser and Smith [7] and Lekić and Kok [9]. In common with these studies, the wall temperature was considered constant throughout the simulation. The wall temperature measured for the gas spring experiment during steady-state periodic operation was used for this parameter. For mass leakage, the pressure in the crankcase sets a boundary condition. The crankcase pressure was assumed to vary isothermally over the course of the cycle.

3.3 Comparison of experimental data and model predictions

Comparison of the experimental pressure profile over a cycle with lumped model predictions (in Fig. *3*) shows good agreement between the two, with closely matched maximum and minimum cylinder pressures, and a well-matched crank angle at which peak pressure occurs (1.6° before TDC).

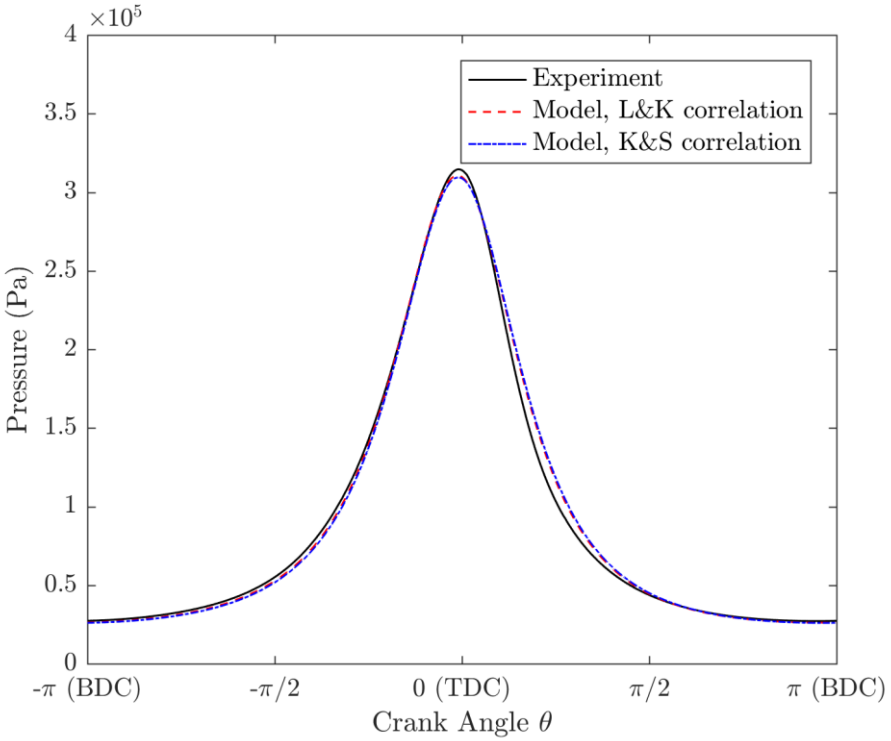

Fig. 3. Cylinder pressure plotted against crank angle from the experiment and predicted by the lumped model for a run at 109.3 RPM

The net cyclic work-loss is given by Eq. (11), and arises because of heat transfer to and from the cylinder walls, and mass leakage, with the overall effect that the work done to compress the gas is not fully recovered during expansion. The experiment shows in general slightly higher pressures during the compression stroke and lower pressures during the expansion stroke, relative to the models. This corresponds to a slightly larger net cyclic work loss in the experiment.

$$W_{\text{loss}} = \oint P \, \mathrm{d}V \, . \tag{11}$$

Beyond the net cyclic loss, the time-resolved measurements of pressure, temperature and volume can be used to obtain the instantaneous losses, in particular the instantaneous gas-to-wall heat transfer, $\dot{Q}_{\text{w}}$, by means of the energy conservation equation (Eq. (2)) applied to the cylinder.

Fig. 4 shows the gas-to-wall heat flux over a cycle from the experimental and model runs. Agreement is broadly good, with the heat flux profile qualitatively well represented by the model. The experimental data shows a larger negative heat flux (transfer from gas to wall), particularly at TDC. The phase shift between the crank angle at maximum heat transfer rate and TDC is also larger for the experiment. The experiment also exhibited greater heat transfer from the wall to the gas before and after BDC (crank angles between π/2 and –π/2).

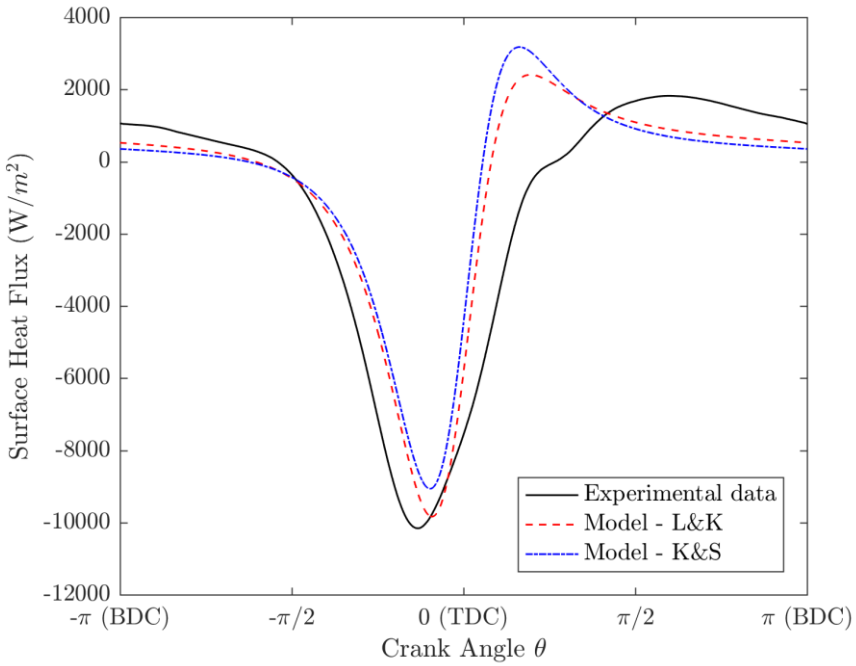

Fig. 4. Surface heat flux re-sampled on the crank angle from the experimental and predicted by the model for a run at 109.3 RPM

Two key modelling assumptions are relevant to these issues. The first is that the lumped-mass model assumes a constant, uniform wall temperature. Though this is a commonly made assumption, sidewall measurements using micro-thermocouples have indicated local wall temperature variations of more than 5 K, and cylinder head variations are likely to be larger still. The second, and likely more significant, is that the heat transfer correlations used were developed for an idealised gas spring, at low compression ratio and without mass leakage. In reality, the mass intake/exhaust through the piston rings will affect the thermal boundary layer close to the piston face, though the magnitude of this effect will require further work to isolate.

The net cyclic work loss has previously been defined as the sum of net losses associated with mass leakage and heat transfer. Having established the heat flux over a cycle, the contribution of the latter component can be identified using the net cyclic heat loss:

$$Q_{\text{loss}} = \int \dot{Q}_{\text{w}} \, \mathrm{d}t \, . \tag{12}$$

The total non-dimensional loss, ψ_{total}, is obtained by normalising the net cyclic work loss by the average of the compression and expansion work. Similarly, the thermal cyclic loss, ψ_{therm}, is given by normalising the net cyclic heat loss by the same factor.

$$\psi_{\text{total}} = \frac{W_{\text{loss}}}{\frac{1}{2}\oint |P\,\mathrm{d}V|} \text{ and } \psi_{\text{therm}} = \frac{Q_{\text{loss}}}{\frac{1}{2}\oint |P\,\mathrm{d}V|}\,. \tag{13}$$

Calculating these parameters for experimental and model runs over a range of frequencies leads to Fig. 5. The cyclic losses are plotted against Péclet number, Pe_ω, a non-dimensional oscillation frequency defined as:

$$Pe_\omega = \frac{\omega {D_\text{h}}^2}{4\alpha_\text{m}}\,. \tag{14}$$

where ω is the angular frequency, D_h is the mean hydraulic diameter (4 × volume / surface area) and α_m is the mean thermal diffusivity over a cycle.

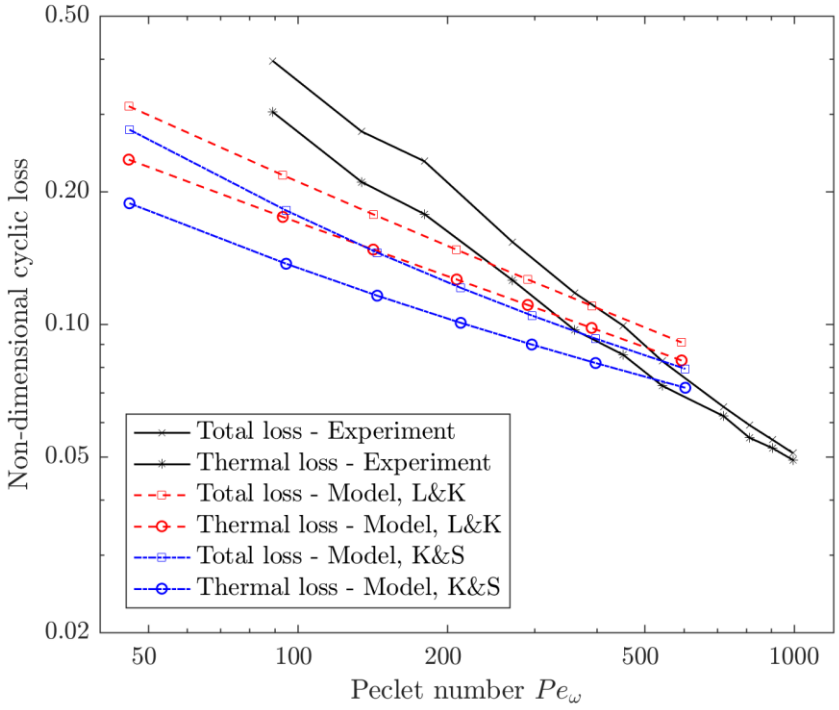

Fig. 5. Total and thermal cyclic losses as a function of Péclet number, plotted for experimental runs and for lumped model simulations using the Lekić and Kok, and Kornhauser and Smith (KS) heat transfer correlations; note the log-log scale

Fig. 5 shows some agreement between experiment and lumped model loss predictions, with both showing total and thermal loss declining with increasing the non-dimensional frequency, Pe_ω. The proportion of the total loss resulting from the thermal loss is also seen to increase with increasing frequency, as the proportion of total loss associated with mass leakage correspondingly falls. This is to be expected: higher oscillation frequencies result in lower time for mass leakage to occur.

4. Performance maps of the reciprocating-piston expander

In this section, the model is used to predict the thermodynamic performance of a reciprocating-piston expander with a rotary valve system. The dimensions of the system considered are the following: the bore diameter is 60 mm, the stroke length is 57 mm, the connecting-rod length is 148.5 mm, and the dead volume height is 10 mm. The intake starts at TDC and the valve closes 72° later, resulting in a volume intake range $\Delta V_\text{in} = 63$ mL. The exhaust starts at BDC and the exhaust range is 144°. The fluid used is an organic fluid, Pentafluoropropane R245fa, often used in ORC technologies.

The upstream and downstream pressures are considered constant along the cycle. In the results presented below, the exhaust pressure is kept the same, $P_{\text{out}} = 1.5$ bar, while the intake pressure is varied to study different pressure ratios. The piston oscillation frequency is also varied in order to draw performance maps, where the power output $\dot{W}$ (Fig. 6) and the expander efficiency η (Fig. 7) are plotted against the oscillation frequency and the pressure ratio. This latter is defined as:

$$\eta = \frac{\dot{W}}{\dot{m}(h_{\text{in}} - h_{\text{out}}^{\text{is}})}, \tag{15}$$

where h_{in} is the gas enthalpy at the intake (or upstream) of the expander and $h_{\text{out}}^{\text{is}}$ is the isentropic exhaust enthalpy defined as the gas enthalpy at the exhaust pressure, P_{out}, and at the intake specific entropy, S_{in}:

$$h_{\text{out}}^{\text{is}} = h(P_{\text{out}}, S_{\text{in}}) . \tag{16}$$

Fig. 6 shows that the power output increases both with the rotational speed of the engine and with the imposed pressure ratio, which is expected. With increasing the intake pressure (and thus the pressure ratio), the pressure applied on the piston increases and so does the produced work. Increasing the oscillation frequency of the piston also logically increases the produced power, while it is observed that the power does not increase much at high RPMs for a given pressure ratio.

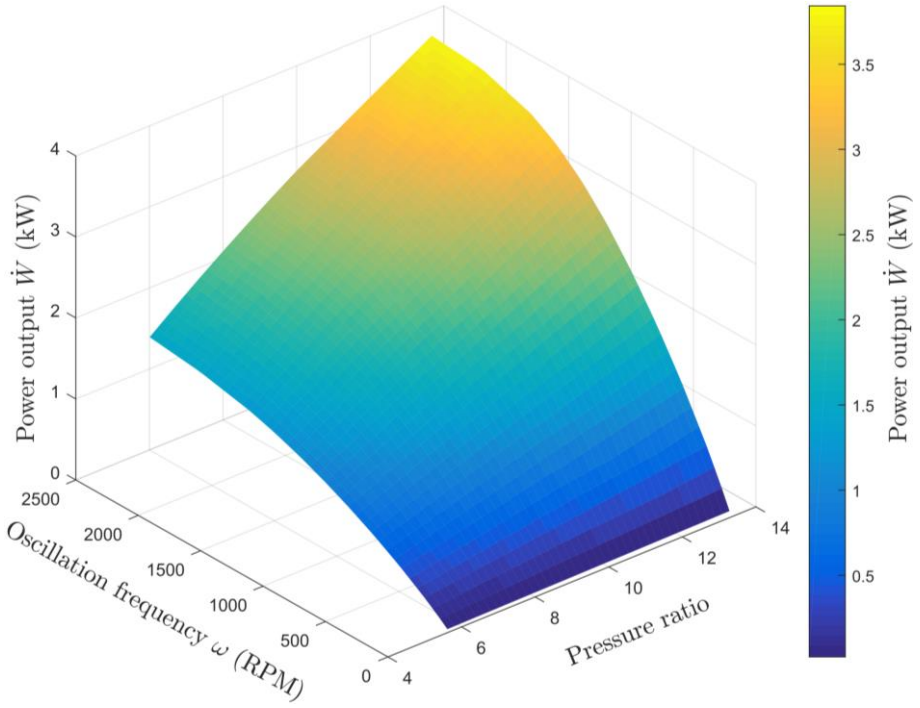

Fig. 6. Performance map plotting the power output as a function of the pressure ratio and the oscillation frequency

Fig. 7 shows that the expander efficiency, unlike the power output, decreases with increasing the pressure ratio. This denotes higher losses at higher pressure ratios. In Fig. 7 we can also observe that for a given pressure ratio, the expander efficiency first increases with the oscillation frequency, reaches a maximum and then decreases. This is due to the pressure losses through the valves. At high RPMs, the valve opening time is reduced and less time is left for the high pressure gas to fill the expansion chamber. As a result, the maximum pressure reached in the chamber diminishes with increasing RPMs, and the efficiency drops. Increasing RPMs also has another effect. As noticed above, less time is left for the high pressure gas to fill the expansion chamber. Hence, the resulting cyclic mass flow rate, $\dot{m}_{\text{c}}$, moves away from the maximum achievable rate, $\dot{m}_{\text{max}}$, defined as:

$$\dot{m}_{\text{max}} = \frac{(\rho_{\text{in}} - \rho_{\text{TDC}})\, V_{\text{TDC}} + \rho_{\text{in}} \Delta V_{\text{in}}}{t_{\text{c}}} . \tag{17}$$

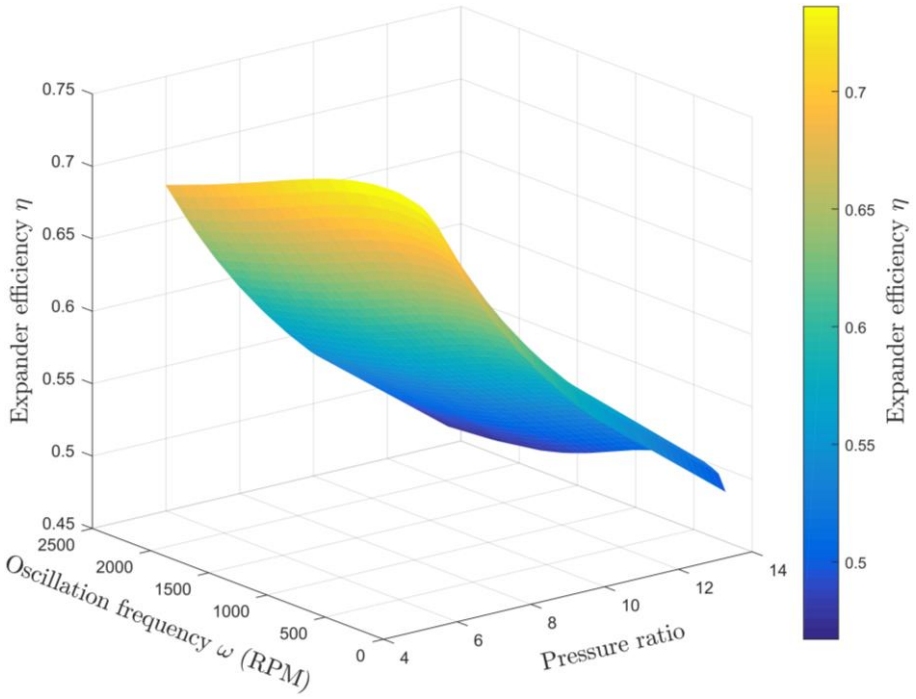

Fig. 7. Performance map plotting the expander efficiency η as a function of the pressure ratio and the oscillation frequency.

This effect can be measured with the volumetric efficiency, defined as:

$$\eta_{\mathrm{vol}} = \frac{\dot{m}_{\mathrm{c}}}{\dot{m}_{\mathrm{max}}}. \tag{18}$$

In Fig. 8, the volumetric efficiency, η_{vol}, is plotted against the oscillation frequency. The drop in η_{vol} while increasing ω is similar for all the studied pressure ratios and intensifies for RPMs higher than approximately 1250.

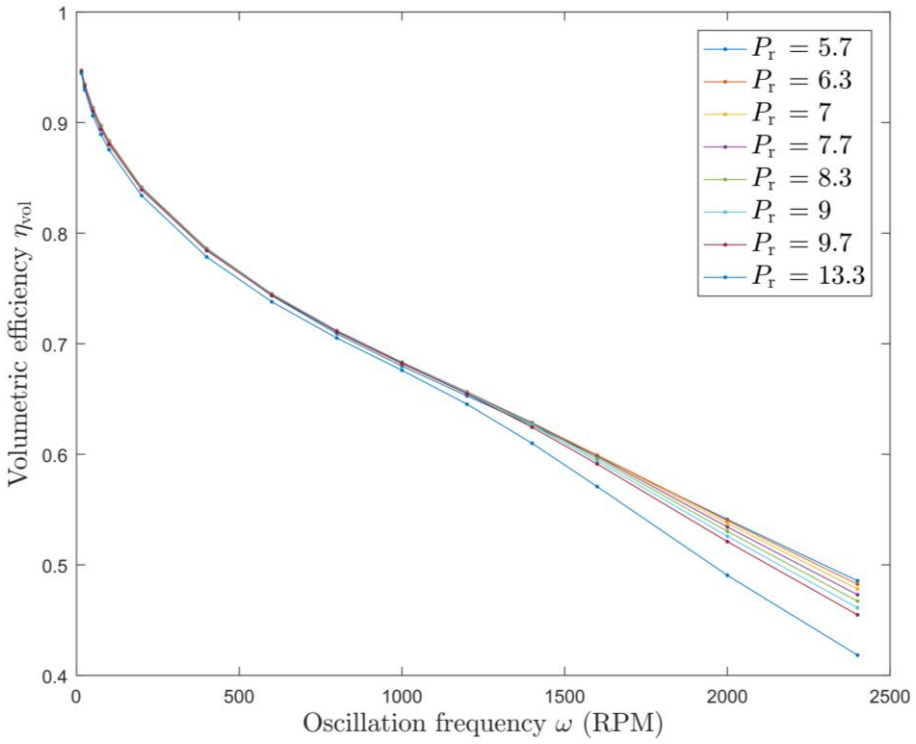

Fig. 8. Volumetric efficiency as a function of the oscillation frequency for different pressure ratios

5. Conclusion

In this paper, we presented an analysis and quantification of the three main loss mechanisms observed in reciprocating-piston compressor or expander machines by employing a lumped dynamic model. The model accounts for pressure drops through the valves, unsteady gas-to-wall in-cylinder heat transfer, and mass leakage to the crankcase through the piston rings. The model is suitable for a wide range of applications as it includes real gas effects by interpolating thermo-physical properties in the NIST database. The model has been compared to experimental data obtained on a gas spring and general good agreement is observed. The heat losses though seem to be underestimated by the model that is based on correlations developed for an idealised gas spring, at low compression ratio and without mass leakage. The validity of these correlations in realistic reciprocating-piston devices is questionable. Finally, the model is used to generate performance maps of an expander that can be used as part of design tools for specific applications.

Acknowledgements

This work was supported by the UK Engineering and Physical Sciences Research Council (EPSRC) [grant numbers EP/P004709/1 and EP/J006041/1]. Data supporting this publication can be obtained on request from cep-lab@imperial.ac.uk.

References

[1] White A.J., Parks G., Markides C.N., Thermodynamic analysis of pumped thermal electricity storage. Applied Thermal Engineering. 2013; 53(2): 291-298.

[2] Mathie R., Markides C.N., White A.J., A framework for the analysis of thermal losses in reciprocating compressors and expanders. Heat Transfer Engineering. 2014; 35(16-17): 1435-1449.

[3] Heywood J.B., Internal Combustion Engine Fundamentals: McGraw-Hill Education; 1988.

[4] Rakopoulos C.D., Kosmadakis G.M., Dimaratos A.M., Pariotis E.G., Investigating the effect of crevice flow on internal combustion engines using a new simple crevice model implemented in a CFD code. Applied Energy. 2011; 88(1): 111-126.

[5] Pfriem H., Periodic heat transfer at small pressure fluctuations. ; 1943.

[6] Overbye V.D., Bennethum J.E., Uyehara O.A., Myers P.S., Unsteady heat transfer in engines. SAE Technical paper; 1961.

[7] Kornhauser A.A., Smith J.L., Application of a complex Nusselt number to heat transfer during compression and expansion. Journal of heat transfer. 1994; 116(3): 536-542.

[8] Lekic U., Kok J.B.W., Heat transfer and fluid flows in gas springs. Open Thermodynamics Journal. 2010; 4: 13-26.

[9] Lekic U., Fluid flow and heat transfer in a helium gas spring-computational fluid dynamics and experiments: PhD, University of Twente; 2011.

[10] Mathie R., White A.J., Markides C.N., Ultrasonic measurements of unsteady heat transfer in a reciprocating gas spring. In International Conference on Heat Transfer, Fluid Mechanics and Thermodynamics; 2014.